

*Accepted March 7th 2024***Double-Diffusive Thermo-Solutal Hadley-Prats Flow: Stability Analysis***Muhammed Rafeek K. V¹, G. Janardhana Reddy^{1,*}, Anjanna Matta², Hussain Basha^{3,*} and O. Anwar Bég⁴**¹Laboratory on Computational Fluid Dynamics, Department of Mathematics, Central University of Karnataka, Kalaburagi, India.**²Department of Mathematics, Faculty of Science & Technology, The ICFAI Foundation for Higher Education, Hyderabad, India.**³Department of Mathematics, Government Degree College, Sindhanur-584128, Karnataka, India.**⁴Professor and Director-Multi-physical Engineering Sciences Group (MPESG), Aeronautical/Mechanical Engineering Department, Corrosion/Coating Lab, SEE Bldg, Salford University, Manchester M54WT, UK.***Corresponding Authors; E-mails: gjr@cuk.ac.in, hussainbmaths@gmail.com***Abstract**

A mathematical model is developed to study the onset of double-diffusion fluid flow through an infinite permeable channel with internal heat source and viscous dissipation effects under the influence of convection conditions. Darcy's model is utilized for the considered isotropic and homogenous porous medium. A linear instability analysis is conducted and the longitudinal roll disturbances are examined. The dimensionless emerging eigenvalue problem is solved numerically using the fourth order Runge-Kutta scheme for longitudinal roll disturbances. Critical values of wave number and vertical thermal Rayleigh number are determined. A higher value of Gebhart number is observed to correlate significantly with the destabilizing phenomena in Hadley-Prats flow. Concentration based internal heat generation also strongly modifies the critical thermal Rayleigh number. Also, it is found that, the horizontal mass flow and viscous dissipation exert a substantial influence on the onset of instability in the flow regime. Linear instability analysis indicates that, greater values of Lewis number in the porous medium stabilize the convection process for both values of mass diffusion parameter (C_z). Enhancing C_z from negative to positive

values diminishes the critical thermal Rayleigh (R_z) value and consequently induces instability in the porous medium. Increased concentration-based internal heat generation generates the destabilisation process in the flow region. Extensive visualization and interpretation of the solutions relating to the onset of convection are provided. The study is relevant to geothermal, industrial manufacturing and chemical engineering transport processes.

Key-Words: Thermo-convective instability; eigenvalues; critical wave number; Gebhart number; Lewis number; Rayleigh number; concentration-based internal heat generation; mass diffusion; geothermic.

1. Introduction

Double diffusive (or thermohaline, if heat and salt are involved) thermo-convective instability in a horizontal infinite porous layer (material consisting of a solid with an interconnected void) saturated with the fluid has numerous applications including geothermal reservoirs Chen et al. [1], underground energy transport Bendrichi and Shemilt [2], groundwater transport Straughan [3], chemical engineering micro- or nano-scale devices Anderson et al. [4], oil recovery Taslim and Narusawa [5], food processing, nuclear reactors cooling, waste disposal of nuclear reactors, thermal convection in clouds etc. In many of these systems, concentration-based internal heat generation with viscous dissipation (internal friction) effect contributes significantly. The important effects in thermohaline convection mechanism arise due to the rapid heat diffusion than the dissolved substances (species). However, in practical applications, the fluid layer was steadily and uniformly illuminated with light emitted by a sodium vapour lamp. This radiation acted as an internal heat source. Moreover, the above-mentioned convection mechanism is penetrative, which is modelled via an internal heat source. If concentration based internal heat source is implemented to the porous medium region, it gives the system which is equivalent in model such as salt gradient layer in solar pond. Usually, this type of convection process arises in sea water flow and mantle flow in the earth's crust. In these applications, the porous medium is frequently simulated as a Darcian regime in which the flow is highly viscous and inertial effects are negligible. Further, many complex characteristics arise in such flows including linear and nonlinear hydrodynamic stability analysis, convection rolls, oscillatory behavior, thermal stratification, thermal dispersion, anisotropic percolation etc. A subset of these flows, known as 'Hadley-Prats flows,' was introduced

in the eighteenth century by George Hadley, a meteorologist, who provided a comprehensive framework for the dispersion of airstreams in atmospheric media. The fluid motion produced at the central regime of a porous regime in the neighborhood of the liquid layer due to the thermal differences in one dimensional flow can be formulated in terms of the Navier-Stokes equations. Later, thermal convection between two parallel infinite horizontal porous layers caused by temperature variations in the middle of the boundaries was examined by Horton and Rogers [6] and Lapwood [7] in their seminal studies and these investigations became the benchmarks for the thermo-convective hydrodynamic stability simulations.

Mono-diffusive convection between two horizontal parallel porous layers with internal heat generation has attracted the attention of many investigators. In this direction, the comprehensive linear instability analysis was discussed by Nield [8]. Further, the Nield's analysis was extended by various researchers to incorporate the impact of viscous dissipation on transport characteristics. However, relatively few researchers were examined the thermal convection instability with the collective consequences of the viscous dissipation and internal heat generation effect. In this direction, the following are the available investigations on the physical problem considered above, as reported in the literature. Barletta et al. [9] described the case of inclined infinite horizontal porous layers suspended between two parallel isothermal boundaries with an internal heat generation effect. A linear instability analysis provides the adequate reasons for the disturbances of classical flow under the steady state conditions to be destabilized. Nield and Bejan [10] documented the practical applications of thermal instability analysis in porous medium for a range of various physical parameters in their monographs. Hill [11] examined the thermo-solutal instability in the horizontal porous layers by considering internal heat generation as a function of concentration. Weber [12] significantly studied the thermal instability analysis for vertical and horizontal thermal gradients, although this study confined to small horizontal thermal gradients only. However, the thermal convection analysis of double diffusive flow mechanism in permeable porous medium was elaborately discussed by Ingham and Pop [13], Vafai [14] and Nield and Bejan [10]. Mono-diffusive non-homogeneous flow with imposed thermal conditions at the walls induced due the basic flow (termed as Hadley-Prats flow) was studied by Weber [12] and Nield et al. [15]. Additionally, Nield et al. [15] analyzed the double diffusive saturated Hadley fluid flow under the inclined solutal and thermal gradients in an infinite horizontal porous layer. An extension of this study with horizontal mass flow was described by Manole et al. [16]. Barletta and Nield

[17] described the Hadley-Prats flow by considering horizontal concentration diffusion mechanism under inclined temperature gradients. These investigations correspond to the linear instability analysis including computation of critical physical parameter values controlling the flow characteristics in the complex flow systems including porous media with small porosity. Matta et al. [18] investigated the double diffusive Hadley-Prats flow with mass diffusion-based internal thermal generation in an infinite horizontal porous layer. Also, Matta et al. [19] studied the effect of gravitational field on the thermo-convective stability analysis.

Viscous dissipation effect associated with frictional heating in fluids arises in many of the industrial processes including both internal and external convection flows such as thermal mixing devices, boundary layer coating systems, bioreactors, polymer processing, geochemical reservoir behaviour, proposed hydrogen storage in saline geological repositories etc. Viscous dissipation effect is significant in real viscous fluids and its inclusion therefore furnishes more accurate appraisal of the heat transfer behaviour in engineering problems. Real fluids exhibit energy losses through molecular collisions leading to the internal friction. The majority of convective fluid flow problems in horizontal porous layer are due to the temperature gradients in the middle of the boundaries and contribute to the resulting fluid flow instability. Thus, viscous dissipation effect is critical for the fluid flow problems in which there is not an external temperature gradient across the parallel boundaries for which the case of an infinite Brinkman parameter was used. Important studies on viscous heating (dissipation) in the thermal convection flows have been reported by Barletta and Nield [17, 20] and dissipation concept was extended to boundary layer studies by Gebhart [21]. Turcotte et al. [22] described the effect of viscous dissipation on the Bénard convection with an adiabatic temperature gradient. Their investigation meticulously described that, the presence of viscous dissipation effect significantly decreases the fluid motion and induces the stability. The thermo-convective flow features of Hadley-Prats fluid flow in a porous medium was reported by Barletta and Storesletten [23], Nield et al. [24], Barletta and Nield [25], Deepika and Narayana [26]. These studies showed that, the stability induced through viscous heating can be originated even in the absence of thermal buoyancy forces in a porous medium. Deepika and Narayana [27] described the linear stability analysis for the double diffusive flow with viscous dissipation effect through porous medium filled with Newtonian fluid. The study of viscous dissipation consequences in free convective flow is noteworthy in a range of devices that are related to a greater rotational velocity and gravitational field and in higher length scale problems.

However, when viscous dissipation effect involves, the temperature profile becomes nonlinear and due to this the boundary layer flow characteristics were modified and which in turn can influence the central flow characteristics. Ene and Sanchez-Palencia [28] discussed the viscous dissipation effect through energy equation and showed that, the dissipation effect is minimum but not negligible in case of natural convection flows. Many investigations including [23-29] have carefully studied the influence of viscous dissipation effect on fluid flow with stability analysis.

Thirlby [30], Tveitereid and Palm [31] elaborately studied the thermal convection flow mechanism with internal heat generation effect with various physical conditions. In many of the practical applications, one can find that, the fluid layer being steadily and uniformly illuminated with light (thermal radiation) emitted by a sodium vapour lamp from above, in this case radiation acts as an internal heat source. However, the convection mechanism mentioned above is penetrative and can be modeled using the concept of an internal heat source. Internal heat sources can also arise in materials fabrication via localized heat spots and furthermore in geophysical/geothermal flows where the earth's mantle is heated internally. Schwiderski and Schwabh [32] and Tritton and Zarraga [33] provided limited results related to the experimental analysis of heat generation effects. Parthiban and Patil [34] analyzed the thermal instability with uncertain heated boundaries in the presence of heat generation and inclined thermal gradients. Parthiban and Patil [35] extended their investigation by considering an anisotropic porous layer with uniformly distributed internal heat generation. Their analysis was carried-out by deploying Galerkin scheme to model the influence of temperature gradients in a horizontal channel with non-identical boundaries. Also, showed that, the initial convective process is encouraged with internal heat generation including horizontal temperature gradients and there is a sharp boost in the associated Rayleigh number for the higher values of horizontal thermal gradients. Matta et al. [36, 37] studied the stability analysis on the thermal convection flow mechanism with mass flow and gravity variation effects. Also, Matta et al. [18] and Deepika et al. [38] discussed the effects of concentration-based internal heat generation on the thermal convection flow mechanism.

The main aim and objective of this study is to examine the stability aspects of double diffusive Hadley-Prats flow in a porous medium with concentration-based internal heat generation, mass flow, temperature gradient and viscous dissipation effects. The considered physical effects were generalizes the previous studies of Krishnamurti [39] and Hill [11]. Krishnamurti [39] and Hill [11] flow models have gained widespread usage in modern geophysical fluid dynamics,

notably in the study of cumulus cloud convection. Kaloni and Qiao [42-44] extensively studied the Hadley-Prats nonlinear convection flow problems with different physical effects by using energy method. Also, Kaloni and Lou [45] studied the energy method to investigate nonlinear stability analysis for the viscoelastic fluid. Reshmi and Murthy [46] studied the onset of convective instability analysis of horizontal throughflow in a porous layer with inclined thermal and solutal gradients. Bhadauria [47] discussed the influence of internal heat source on the double-diffusive convection flow in a saturated porous layer under anisotropic conditions. Yadav et al. [48] explored the new flow model that deals with the effect of thermal conductivity and viscosity variations on the onset of double-diffusive nanofluid convection in a rotating porous medium layer. Yadav and Wang [49] described the convection thermal transport mechanism in a heat producing porous layer filled with a non-Newtonian fluid under nanofluid properties. Yadav [50] discussed the buoyancy-motivated onset of convective nanofluid flow through an anisotropic porous layer with variable gravity and internal heating via numerical scheme. Capone et al. [51] described the influence of internal heating on the double-diffusive penetrative convective fluid flow through an anisotropic porous layer with throughflow. Yadav et al. [52] demonstrated the influence of convective double diffusion mechanism on the non-Newtonian Kuvshiniski fluid flow through a reactive porous layer. Similar study is performed by Yadav et al. [53] with Maxwell fluid under chemical reaction conditions. These investigations involve the parallel plate geometry with saturated porous medium (Darcy's model) through linear instability analysis. The inclusion of concentration-based internal heat source is justified as it provides a good approach for considering salt gradient layers in geothermal and solar pond energy applications. Double diffusive convection enables the simultaneous consideration of heat and mass (species, e.g. salt) transfer induced by buoyancy effects. The general conservation equations are presented and then non-dimensionalized and converted into a robust eigenvalue problem with associated boundary conditions. Numerical solutions are obtained via Runge-Kutta (RK) scheme with shooting method. Particularly, viscous and concentration-based internal heat source on the onset of convection in double-diffusive Hadley-Prats flow is addressed.

2. Mathematical formulation

The considered physical configuration consists of a homogeneous infinite horizontal porous layer filled with a saturated Newtonian fluid between two iso-solutal and isothermal immovable plates separated by distance d . The tortuosity, non-Darcy, geochemical reaction and

thermal stratification effects are neglected. The considered porous medium is rigid (non-deformable). The upward vertical axis is z' and the horizontal axes are x' and y' . The inlet flow velocity is u_0 in the x' -direction. The plates therefore occupy the $x'y'$ plane. The imposed horizontal temperature and solutal gradients are $(\beta_{\theta_x}, \beta_{\theta_y})$ and $(\beta_{C_x}, \beta_{C_y})$ with internal heat source Q' . However, the physical model is depicted in **Fig. 1**.

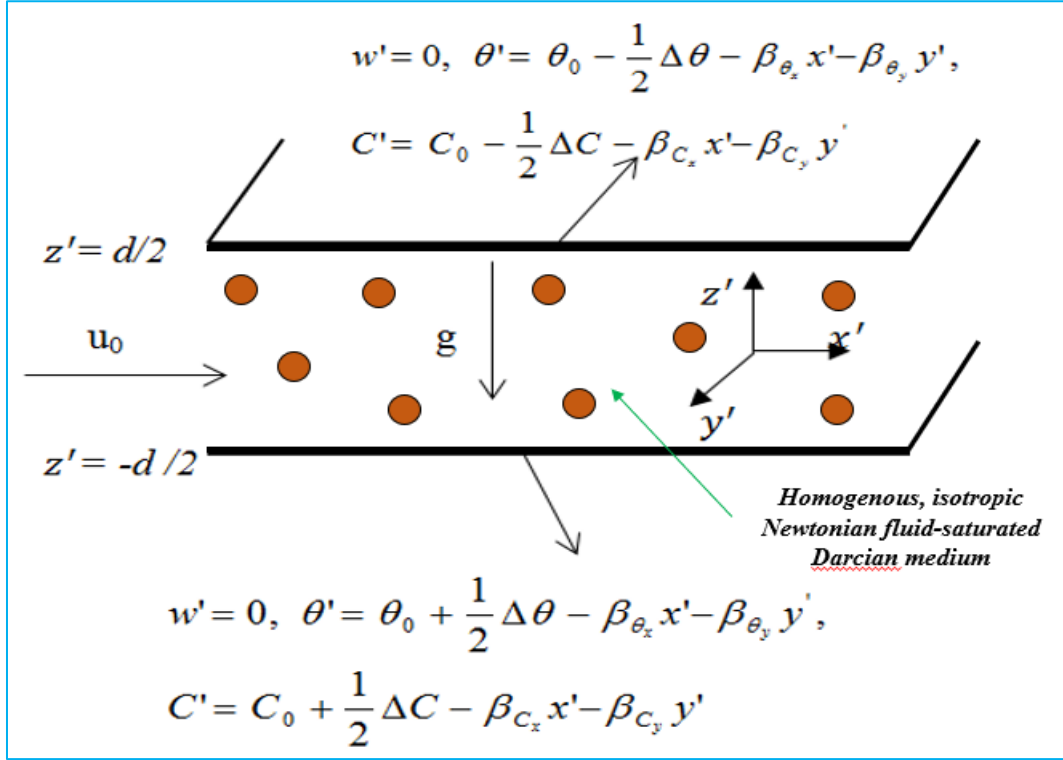


Figure 1. The physical problem and coordinate system.

A homogeneous concentration variation ΔC and normal thermal variation $\Delta\theta$ were considered at the horizontal boundaries of the channel. Temperature and concentration of the fluid varies from point to point when fluid flows between infinite horizontal porous parallel plates. Linear Oberbeck-Boussinesq approximations (density deviations are such that, they are sufficiently small and can be neglected with the exclusion of the buoyancy force terms) and Darcy's law is deployed for the considered porous medium. The density ρ'_f of the fluid is obtained through the well-defined equation $\rho'_f = \rho_o[1 - (\theta' - \theta_o)\gamma_\theta - (C' - C_o)\gamma_C]$, where θ' is the temperature, C' is the species concentration, γ_C and γ_θ are coefficients of species and temperature gradients, ρ_o is the density when mass diffusion is C_o and temperature difference is θ_o . With these

assumptions, the representative transport equations for mass, momentum, species concentration (solutal diffusion) and heat (energy) of the considered physical problem with Darcy body force, viscous heating and concentration-based internal heat generation are defined as follows [18, 19, 36, 37, 42, 43, 44, 45]:

$$\nabla' \cdot q' = 0, \quad (2.1)$$

$$\frac{\mu}{K} q' + \nabla' P' - \rho'_f g k = 0, \quad (2.2)$$

$$\phi \left(\frac{\partial C'}{\partial t'} \right) + q' \cdot \nabla' C' = D_m \nabla'^2 C' \quad (2.3)$$

$$(\rho c)_m \frac{\partial \theta'}{\partial t'} + (\rho c_p)_f q' \cdot \nabla' \theta' = k_m \nabla'^2 \theta' + (\rho c_p)_f \frac{\vartheta}{K c} q' \cdot q' + Q'(C' - C_0), \quad (2.4)$$

where Eq. (2.1) denotes the incompressibility condition (conservation of mass). Further, the conditions on the horizontal boundaries are defined as follows [18, 19, 36, 37, 42, 43, 44, 45]:

$$\left. \begin{aligned} z' = -\frac{1}{2}d: w' = 0, C' = C_0 + \frac{\Delta C}{2} - \beta_{c_x} x' - \beta_{c_y} y', \theta' = \theta_0 + \frac{\Delta \theta}{2} - \beta_{\theta_x} x' - \beta_{\theta_y} y' \\ z' = \frac{1}{2}d: w' = 0, C' = C_0 - \frac{\Delta C}{2} - \beta_{c_x} x' - \beta_{c_y} y', \theta' = \theta_0 - \frac{\Delta \theta}{2} - \beta_{\theta_x} x' - \beta_{\theta_y} y' \end{aligned} \right\} \quad (2.5)$$

In the above Eqs. (2.1)-(2.5), the seepage (Darcy velocity or superficial velocity, also known as the filtration velocity) velocity vector is $q' = (u', v', w')$, P' denotes the pressure, subscripts f and m designate respectively the fluid and porous medium. Additionally, μ , c , k_m , D_m , g , K , k , ϑ , ϕ , c_p and ρ_0 represent the dynamic viscosity, specific heat of solid, thermal conductivity, solutal (molecular) diffusivity, gravitation field, isotropic permeability of porous medium, vector along z' -direction, kinematic viscosity, porosity of the medium, specific heat of fluid and density of the fluid medium. The following dimensionless variables and parameters are now invoked [18, 19, 36, 37, 42, 43, 44, 45]:

$$\left. \begin{aligned} (x, y, z) = \frac{1}{d} (x', y', z'), \quad t = \frac{\alpha_m t'}{ad^2}, \quad (u, v, w) = q = \frac{dq'}{\alpha_m}, \quad P = \frac{K(P' + \rho_0 g z')}{\mu \alpha_m} \\ \theta = \frac{R_z(\theta' - \theta_0)}{\Delta \theta}, \quad C = \frac{C_z(C' - C_0)}{\Delta C}, \quad Q = \frac{d^2 Q' R_z \Delta C}{k_m \Delta \theta C_z}, \quad \alpha_m = \frac{k_m}{(\rho c_p)_f}, \quad a = \frac{(\rho c)_m}{(\rho c_p)_f} \end{aligned} \right\} \quad (2.6)$$

where (x, y, z) represents the dimensionless Cartesian coordinates, t be the non-dimensional time, (u, v, w) indicates the dimensionless velocity components, P be the non-dimensional pressure, θ be the dimensionless temperature, C be the dimensionless solutal concentration, Q be the concentration-based internal heat generation parameter, α_m be the thermal diffusivity of the fluid

and a is defined as the ratio of thermal capacity of the porous medium to the liquid medium. Using the non-dimensional variables defined in Eq. (2.6), the governing Eqs. (2.1)-(2.5) are reduced to the following form:

$$\nabla \cdot q = 0, \quad (2.7)$$

$$q + \nabla P - \left(\frac{1}{Le} C + \theta \right) k = 0, \quad (2.8)$$

$$\left(\frac{\emptyset}{a} \right) \frac{\partial C}{\partial t} + q \cdot \nabla C = \frac{1}{Le} \nabla^2 C, \quad (2.9)$$

$$\frac{\partial \theta}{\partial t} + q \cdot \nabla \theta = \nabla^2 \theta + Ge q \cdot q + QC, \quad (2.10)$$

where ∇ denotes the 'del' operator and ∇^2 is the Laplacian operator. Also, the prescribed dimensionless boundary conditions at the horizontal walls are taken as follows:

$$\left. \begin{aligned} z = -\frac{1}{2}: \quad w = 0, \quad C = \frac{C_z}{2} - C_x x - C_y y, \quad \theta = \frac{R_z}{2} - R_x x - R_y y, \\ z = \frac{1}{2}: \quad w = 0, \quad C = -\frac{C_z}{2} - C_x x - C_y y, \quad \theta = -\frac{R_z}{2} - R_x x - R_y y \end{aligned} \right\} \quad (2.11)$$

In the above Eqs. (2.7)-(2.11), the vertical, horizontal thermal and solute Rayleigh numbers are denoted as R_z , C_z , R_x , R_y , C_x and C_y respectively, Ge represents the Gebhart number, Le indicates the Lewis number, M represents the Peclet number and these parameters are defined as follows:

$$\begin{aligned} R_z &= \frac{\rho_0 g \gamma_\theta K d \Delta \theta}{\mu \alpha_m}, \quad C_z = \frac{\rho_0 g \gamma_c K d \Delta C}{\mu D_m}, \quad R_x = \frac{\rho_0 g \gamma_\theta K d^2 \beta_{\theta x}}{\mu \alpha_m}, \quad C_x = \frac{\rho_0 g \gamma_c K d^2 \beta_{c x}}{\mu D_m}, \quad R_y = \frac{\rho_0 g \gamma_\theta K d^2 \beta_{\theta y}}{\mu \alpha_m}, \\ C_y &= \frac{\rho_0 g \gamma_c K d^2 \beta_{c y}}{\mu D_m}, \quad Ge = \frac{\gamma_\theta g d}{c}, \quad Le = \frac{\alpha_m}{D_m}, \quad M = \frac{u_0 d}{\alpha_m} \end{aligned} \quad (2.12)$$

From the above boundary condition Eq. (2.11), it is evident that, the vertical thermal and solutal Rayleigh numbers appear in boundary conditions in dimensionless form. The conditions on the temperature and concentration at boundaries of both plates physically represent the linear variations in the thermal and concentration fields.

3. Steady state solutions

The Eqs. (2.7)-(2.10) possess the basic steady state solutions subject to the conditions at the horizontal boundaries and which are defined follows:

$$\theta_s = \tilde{\theta}(z) - R_x x - R_y y, \quad C_s = \tilde{C}(z) - C_x x - C_y y, \quad (3.1)$$

$$(u_s, v_s, w_s) = (u(z), v(z), 0), \quad P_s = P(x, y, z) \quad (3.2)$$

The steady state solution produces:

$$u_s = -\frac{\partial P}{\partial x}, \quad 0 = -\frac{\partial P}{\partial y} \quad (3.3)$$

$$0 = -\frac{\partial P}{\partial z} + \left[\frac{1}{Le} (\tilde{C}(z) - C_x x - C_y y) + (\tilde{\theta}(z) - R_x x - R_y y) \right] \quad (3.4)$$

$$D^2 \tilde{C}(z) = -Le [C_x u_s + C_y v_s] \quad (3.5)$$

$$D^2 \tilde{\theta}(z) = -u_s R_x - v_s R_y - Ge(u_s^2 + v_s^2) - Q(\tilde{C}(z) - C_x x - C_y y) \quad (3.6)$$

where, $D = \frac{d}{dz}$, the net mass flow in x -direction is $\int_{-\frac{1}{2}}^{\frac{1}{2}} u(z) dz = M$ and in y -direction is $\int_{-\frac{1}{2}}^{\frac{1}{2}} v(z) dz = 0$. Peclet number M represents the strength of mass flow. Basic steady state solutions are therefore extractable for velocity, thermal and concentration in the porous medium:

$$u_s = \left(R_x + \frac{C_x}{Le} \right) z + M, \quad v_s = \left(R_y + \frac{C_y}{Le} \right) z, \quad w_s = 0, \quad (3.7)$$

$$\tilde{C} = -C_z z + A, \quad \tilde{\theta} = -R_z z + B, \quad (3.8)$$

where in Eq. (3.8), the unknowns A and B are defined as below:

$$A = \frac{\lambda_1}{24} (z - 4z^3) + \frac{MC_x Le}{8} (1 - 4z^2),$$

$$B = \frac{(\lambda_2 - QC_z)}{24} (z - 4z^3) - \frac{MR_x}{8} (4z^2 - 1) + \frac{\lambda_1 Q}{24} \left(\frac{z^5}{5} - \frac{z^3}{6} + \frac{7z}{240} \right) - \frac{QMLEC_x}{8} \left(\frac{z^2}{2} - \frac{z^4}{3} \right) + \frac{5MC_x Le Q}{384} -$$

$$\frac{Ge}{12} \left[\lambda_3 \left(z^4 - \frac{1}{16} \right) + 4M\lambda_4 \left(z^3 - \frac{z}{4} \right) + 6M^2 \left(z^2 - \frac{1}{4} \right) \right],$$

$$\lambda_1 = C_x^2 + C_y^2 + Le(C_x R_x + C_y R_y), \quad \lambda_2 = R_x^2 + R_y^2 + \left(\frac{R_x C_x + R_y C_y}{Le} \right),$$

$$\lambda_3 = \left(\frac{C_x}{Le} + R_x \right)^2 + \left(\frac{C_y}{Le} + R_y \right)^2, \quad \lambda_4 = \left(\frac{C_x}{Le} + R_x \right). \quad (3.9)$$

However, the fluid flow governed by Eq. (3.7) is termed as Hadley-Prats flow.

4. Disturbance equations

In this section, the basic steady state solutions are perturbed as $q = q_s + \bar{q}$, $\theta = \theta_s + \bar{\theta}$, $C = C_s + \bar{C}$, and $P = P_s + \bar{P}$. Replacing these disturbances into the non-dimensional Eqs. (2.7)-(2.10) leads to the subsequent perturbation equations listed as follows:

$$\nabla \cdot \bar{q} = 0, \quad (4.1)$$

$$\bar{q} + \nabla \bar{P} - \left(\frac{1}{Le} \bar{C} + \bar{\theta} \right) k = 0 \quad (4.2)$$

$$\left(\frac{\phi}{a} \right) \frac{\partial \bar{C}}{\partial t} + q_s \cdot \nabla \bar{C} + \bar{q} \cdot \nabla C_s + \bar{q} \cdot \nabla \bar{C} = \frac{1}{Le} \nabla^2 \bar{C}, \quad (4.3)$$

$$\frac{\partial \bar{\theta}}{\partial t} + q_s \cdot \nabla \bar{\theta} + \bar{q} \cdot \nabla \theta_s + \bar{q} \cdot \nabla \bar{\theta} = \nabla^2 \bar{\theta} + Ge(2q_s \cdot \bar{q} + \bar{q} \cdot \bar{q}) + Q\bar{C}, \quad (4.4)$$

In the above Eqs. (4.2)-(4.4), the different terms are defined as follows:

$$\begin{aligned} \nabla C_s &= -(C_x, C_y, C_z - \tilde{A}), \quad \nabla \theta_s = -(R_x, R_y, R_z - \tilde{B}), \quad \tilde{A} = \frac{\lambda_1}{24}(1 - 12z^2) - M C_x Le z, \\ \tilde{B} &= \frac{(\lambda_2 - Q C_z)}{24}(1 - 12z^2) - MR_x z + \frac{\lambda_1 Q}{24} \left(z^4 - \frac{z^2}{2} + \frac{7}{240} \right) - \frac{QMLeC_x}{24}(3z - 4z^3) - \left. \begin{aligned} & \frac{Ge}{3} \left(\lambda_3 z^3 + M\lambda_4 \left(3z^2 - \frac{1}{4} \right) + 3M^2 z \right) \end{aligned} \right\} \end{aligned} \quad (4.5)$$

Further, the conditions at the horizontal boundaries are defined as follows:

$$\bar{w} = 0, \quad \bar{C} = 0, \quad \bar{\theta} = 0, \quad \text{at} \quad z = \mp \frac{1}{2}. \quad (4.6)$$

From these boundary conditions it is clear that, there is no orthogonal flow velocity and no porous medium, thermal and mass diffusion disturbances arising at the boundaries.

5. Linear instability investigation

In this section, the thermal instability is addressed by investigating the linear stability of the system. To perform the linear instability analysis, the non-linear factors and products of disturbances appearing in Eqs. (4.1)-(4.4) are neglected. The linearized disturbance equations are therefore reduced as follows:

$$\nabla \cdot \bar{q} = 0, \quad (5.1)$$

$$\bar{q} + \nabla \bar{P} - \left(\frac{1}{Le} \bar{C} + \bar{\theta} \right) k = 0, \quad (5.2)$$

$$\left(\frac{\phi}{a} \right) \frac{\partial \bar{C}}{\partial t} + q_s \cdot \nabla \bar{C} + \bar{q} \cdot \nabla C_s = \frac{1}{Le} \nabla^2 \bar{C}, \quad (5.3)$$

$$\frac{\partial \bar{\theta}}{\partial t} + q_s \cdot \nabla \bar{\theta} + \bar{q} \cdot \nabla \theta_s = \nabla^2 \bar{\theta} + 2Ge(q_s \cdot \bar{q}) + Q\bar{C}, \quad (5.4)$$

The linearized boundary conditions are taken as follows:

$$\bar{w} = 0, \quad \bar{C} = 0, \quad \bar{\theta} = 0, \quad \text{at} \quad z = \mp \frac{1}{2}. \quad (5.5)$$

Further, the linearized perturbation equations are reduced as follows:

$$\nabla \cdot \bar{q} = 0, \quad (5.6)$$

$$\bar{q} + \nabla \bar{P} - \left(\frac{1}{Le} \bar{C} + \bar{\theta} \right) k = 0, \quad (5.7)$$

$$\left(\frac{\phi}{a} \right) \frac{\partial \bar{C}}{\partial t} + u_s \frac{\partial \bar{C}}{\partial x} + v_s \frac{\partial \bar{C}}{\partial y} - C_x \bar{u} - C_y \bar{v} + \bar{w} (D\bar{C}) = \frac{1}{Le} \nabla^2 \bar{C}, \quad (5.8)$$

$$\frac{\partial \bar{\theta}}{\partial t} + u_s \frac{\partial \bar{\theta}}{\partial x} + v_s \frac{\partial \bar{\theta}}{\partial y} - R_x \bar{u} - R_y \bar{v} + \bar{w} (D\bar{\theta}) = \nabla^2 \bar{\theta} + 2Ge(u_s \bar{u} + v_s \bar{v}) + Q\bar{C}, \quad (5.9)$$

In the above Eqs. (5.6)-(5.9), the values of $D\bar{C}$ and $D\bar{\theta}$ are defined as follows:

$$D\bar{C} = -C_z + \frac{\lambda_1}{24} (1 - 12z^2) - M C_x Le z,$$

$$D\bar{\theta} = -R_z + \frac{(\lambda_2 - Q C_z)}{24} (1 - 12z^2) - MR_x z + \frac{\lambda_1 Q}{24} \left(z^4 - \frac{z^2}{2} + \frac{7}{240} \right) - \frac{QMLe C_x}{24} (3z - 4z^3) - \frac{Ge}{3} \left(\lambda_3 z^3 + M \lambda_4 \left(3z^2 - \frac{1}{4} \right) + 3M^2 z \right). \quad (5.10)$$

Meanwhile, the resulting differential equations are linear and independent. Thus, by adopting a Fourier mode solution technique to Eqs. (5.7)-(5.9) under the presence of boundary conditions Eq. (5.5), we have the following solution format:

$$[\bar{q}, \bar{\theta}, \bar{C}, \bar{P}] = [q(z), \theta(z), C(z), P(z)] \exp\{i(kx + ly - \sigma t)\} \quad (5.11)$$

Eliminating pressure term P from the Eq. (5.7) yields:

$$(D^2 - \alpha^2)w + \left(\frac{C}{Le} + \theta \right) \alpha^2 = 0, \quad (5.12)$$

$$\left(\frac{1}{Le} (D^2 - \alpha^2) + i \left(\frac{\phi}{a} \right) \sigma - iku_s - ilv_s \right) C + \frac{i}{\alpha^2} (kC_x + lC_y) Dw - (D\bar{C})w = 0, \quad (5.13)$$

$$\left. \begin{aligned} & (D^2 - \alpha^2 + i\sigma - iku_s - ilv_s)\theta + \\ & \frac{i}{\alpha^2} (kR_x + lR_y + 2Ge(ku_s + lv_s)) Dw - (D\bar{\theta})w + QC = 0 \end{aligned} \right\} \quad (5.14)$$

The above Eqs. (5.12)-(5.14) with conditions $w = \theta = C = 0$ are satisfied at $z = \frac{1}{2}$ and $z = \frac{-1}{2}$.

The different terms in these Eqs. (5.12)-(5.14) are defined as follows:

$$\begin{aligned}
 D\tilde{C} &= -C_z + \frac{\lambda_1}{24}(1 - 12z^2) - M C_x Le z, \\
 D\tilde{\theta} &= -R_z + \frac{(\lambda_2 - QC_z)}{24}(1 - 12z^2) - MR_x z + \frac{\lambda_1 Q}{24} \left(z^4 - \frac{z^2}{2} + \frac{7}{240} \right) - \left. \begin{aligned} & \frac{QMLeC_x}{24}(3z - 4z^3) - \frac{Ge}{3} \left(\lambda_3 z^3 + M\lambda_4 \left(3z^2 - \frac{1}{4} \right) + 3M^2 z \right) \end{aligned} \right\} \quad (5.15)
 \end{aligned}$$

The eigenvalue problem is therefore defined for the Rayleigh parameter R_z with $\sigma, R_x, R_y, Q, Ge, k, \alpha, \phi, Le, C_x, C_y$ and l as variables. Furthermore $\alpha = \sqrt{k^2 + l^2}$ represents the global wave number and $i = \sqrt{-1}$.

6. Results and discussion

In the previous sections, a linear stability investigation has been conducted to examine the consequences of the viscous dissipation, mass flow, species diffusion and concentration-based internal heat generation effects on the double diffusion Hadley-Prats flow in an infinite horizontal porous layer. The numerical strategy outlined by Barletta and Nield [17, 20] is followed and derived the eigenvalue problem governed by equations (5.12)-(5.14). A linear stability analysis is conducted in which R_z is considered to be an eigenvalue of the stability problem. An ideal Fourier scheme is used to analysis the temperature instability in the Hadley-Prats flow. The critical value of R_z is determined as the minimum value among all the R_z values when α is changed. The matching wave number is defined as the row vector such that $\alpha = (k; l; 0)$. Let consider the stationary convection mechanism obtained by putting $\sigma = 0$ and it was described by Nield [8]. In this case, authors used the non-oscillatory longitudinal technique to study the Hadley-Prats flow. However, the longitudinal perturbations are recorded by setting $k = 0$ in the eigenvalue problem encountered from the stability analysis and results were reported for $k = 0$ and $\sigma = 0$. The stationary longitudinal mode is the only possible mode for the convection induced by horizontal mass flow as stated by Nield and Bejan [10] and Kaloni and Qiao [42, 43, 44, 45]. This result is again reported by Matta et al. [36] by providing the fact that, the imaginary part of σ is zero (the oscillatory mode of convection is does not exist). So the stationary longitudinal mode of convection will give more instability (fluid flow become more unstable) when compared to stationary transverse mode. In the numerical computations, $C_z > 0$ corresponds to the mass

diffusion at the upper boundary exceeding the lower boundary, and $C_z < 0$ indicates the reverse situation. In the present analysis, we took $\frac{\phi}{a} = 1$, $R_y = C_y = 0$ and $Le = 10$. Since, this data is physically consistent with a range of experiments reported in the literature using salt-water/sugar-water based physical systems. The pioneering results have been noticed in the literature of Gebhart et al. [40].

Figures 2 and 3 describe the impact of Peclet number (M) and Gebhart number (Ge) on R_z and R_x with horizontal mass flow for both negative and positive values of C_z in the flow region. In this case, a significant deviation is induced with increasing Gebhart number. Also, a monotonic increase in the vertical Rayleigh number noticed with augmentation in the horizontal Rayleigh number. Figure 2 indicates that, enlarging R_x stabilizes the convection process. Further, M and R_z are decreased by diminishing the Gebhart number Ge . Thus, for a particular value of Ge , the horizontal mass flow stabilizes the fluid flow system.

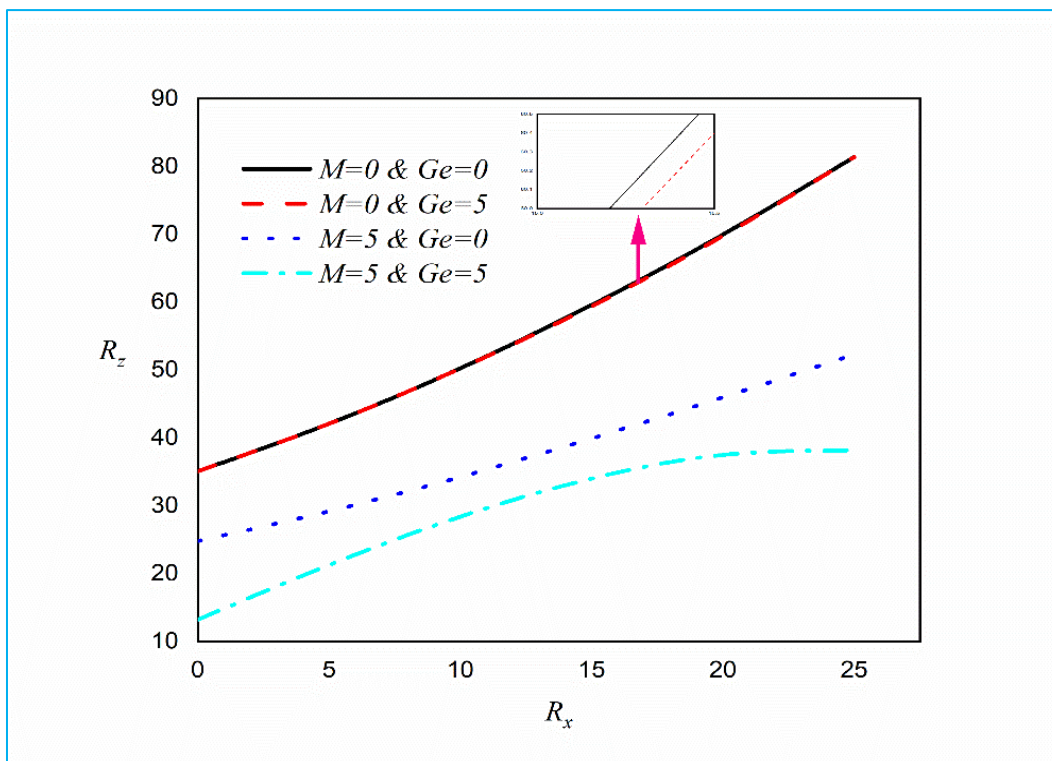


Figure 2: Deviations of R_z against R_x at $C_x = 5$, $R_y = C_y = 0$, $Q = 0$, $Le = 10$ and $C_z = 5$.

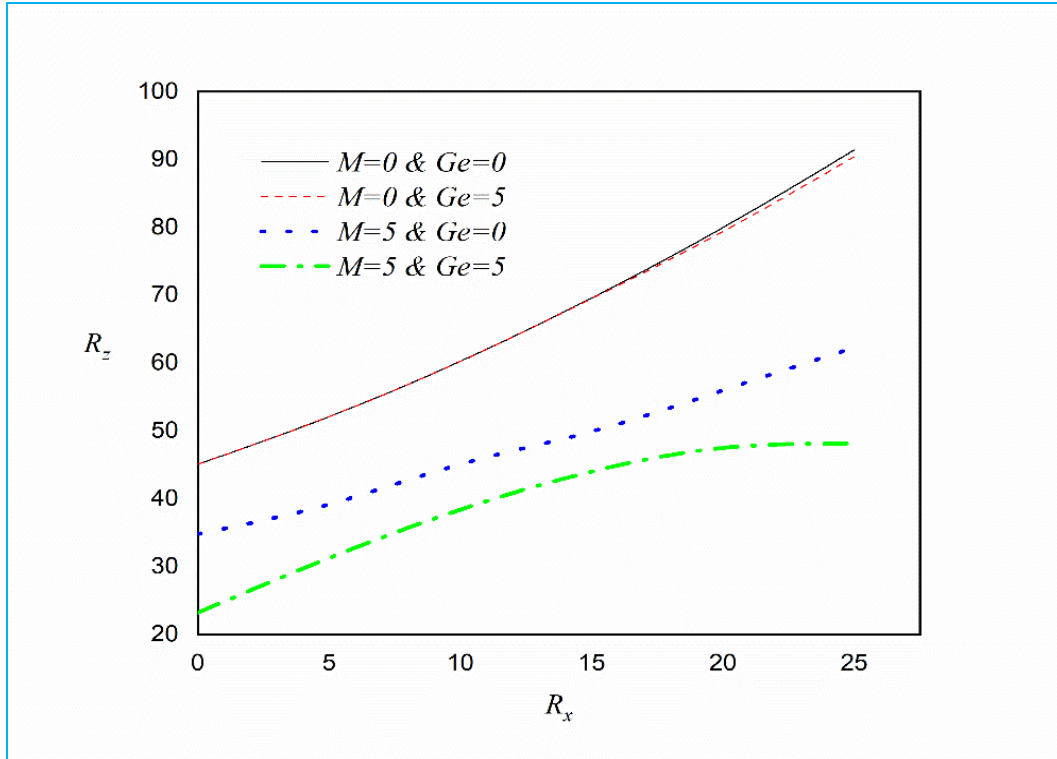


Figure 3: Deviations of R_z with R_x at $C_x = 5$, $R_y = C_y = 0$, $Q = 0$, $Le = 10$ and $C_z = -5$.

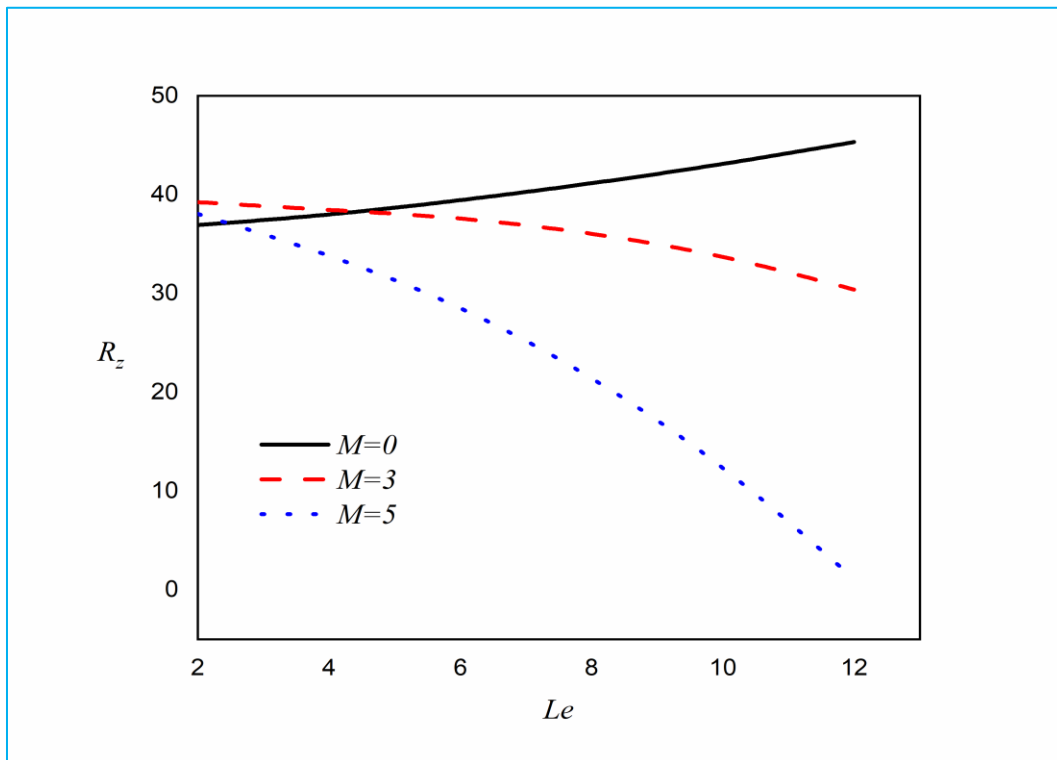


Figure 4: Deviations of R_z with Le at $R_x = C_x = 5$, $R_y = C_y = 0$, $Q = 1$, $Ge = 3$, $C_z = 5$.

Figure 3 indicates the influence of negative value of C_z on the flow process and depicts that the rectilinear instability curves are equivalent to linear stability curves for positive C_z . These observations indicate that, the linear instability calculations provide robust quantitative changes with respect to the horizontal thermal and solutal parameters along with appearance and disappearance of Gebhart number ($Ge = 0$ corresponds to vanishing viscous heating) and M deviations. However there is a sustained increment in critical vertical Rayleigh number (R_z) with increasing horizontal Rayleigh number (R_x). This interaction between vertical and horizontal critical Rayleigh numbers is strongly nonlinear.

Figures 4 and 5 depict the deviations of R_z as function of Le in the presence and absence of mass flow M together with negative and positive values of solutal Rayleigh number C_z . It is important to note that, the Lewis number is the ratio of thermal diffusivity to the mass diffusivity. It is distinct therefore from the more familiar Schmidt number in mass transfer which quantifies the momentum diffusion rate to thermal diffusion rate ratio. Since, we have studied Le , over the range 2 to 12, the implication is that, at the lower limit, the thermal diffusivity is double the mass (molecular) diffusivity whereas at the upper limit thermal diffusivity is dozen times greater than the mass (molecular) diffusivity. This range covers the most of the practical applications in geothermic and chemical engineering [42-46]. Figure 4 indicates that, in the absence of horizontal mass flow ($M = 0$) the critical value of R_z is strongly enhanced as Le rises and the thermo-solutal motion becomes stabilized. Hence, in the presence of mass flow M , R_z is decreased by an elevation in Le for both $C_z < 0$ and $C_z > 0$. The consequence is that, a smaller molecular diffusivity (higher Lewis number) is beneficial for achieving stability in the flow regime. Additionally, it is shown that, the value of R_z is reduced with enlargement in mass flow parameter M . However, the destabilization of Hadley-Prats flow is nevertheless computed for the combined effects of rise in both Lewis number Le and the mass flow parameter M . A linear stability analysis effectively indicates that, the upsurging Lewis number in the porous medium stabilizes the convection process for positive and negative C_z . A similar behaviour is also noticed in Fig. 5. Although an important distinction is that, the negative value of C_z now morphs the $M = 0$ case from linear (Fig. 4) to non-linear, especially at the lower values of Lewis number. However, for $Le > 10$ the linearity is restored in $M = 0$ profile and which illustrated in Fig. 5.

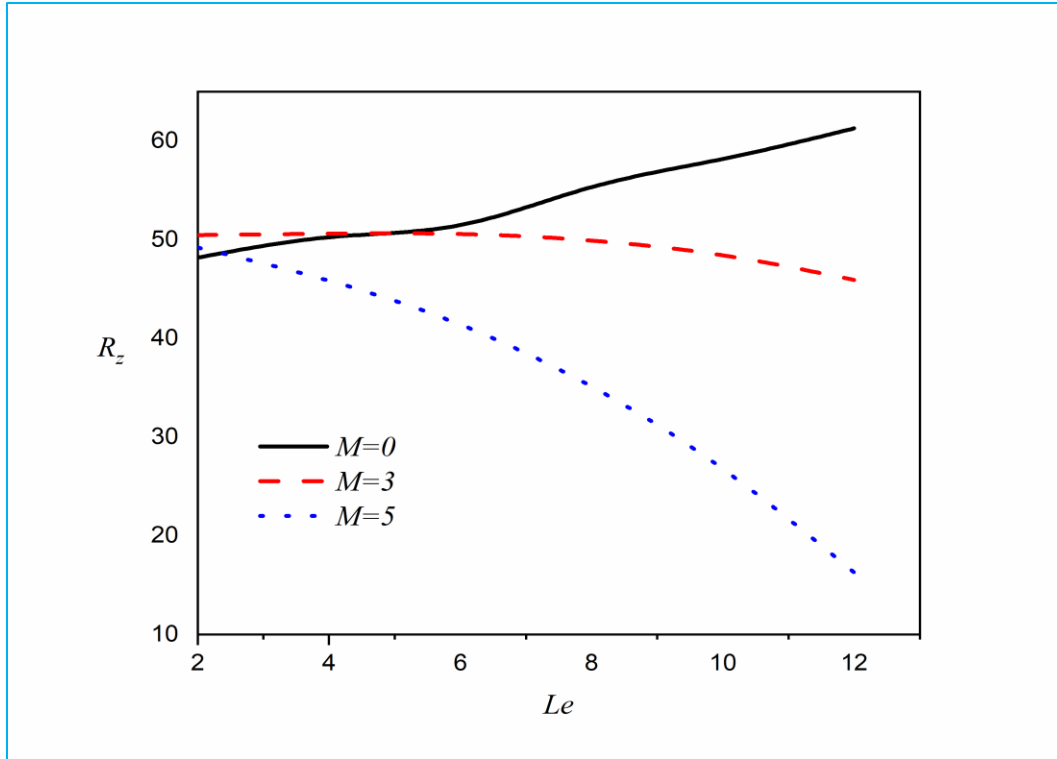


Figure 5: Deviations of R_z with Le at $R_x = C_x = 5$, $R_y = C_y = 0$, $Q = 1$, $Ge = 3$, $C_z = -5$.

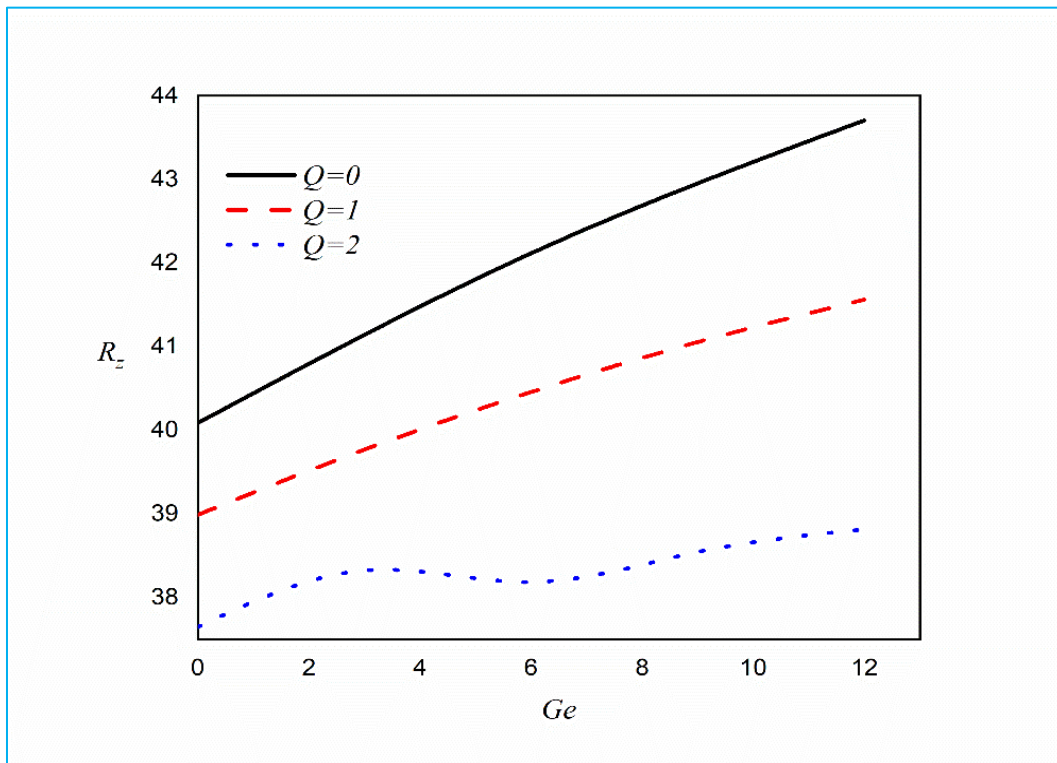


Figure 6: Deviations of R_z with Ge at $R_x = C_x = 5$, $R_y = C_y = 0$, $M = 2$, $Le = 10$, $C_z = 5$.

Figures 6 and 7 demonstrate the influence of internal heat source number Q on vertical Rayleigh number (R_z) and Gebhart number Ge for both positive and negative values of C_z . An increment in concentration based internal heat generation (Q) boosts up the overall temperature of the permeable porous medium. However, with vanishing heat generation ($Q = 0$), the R_z profile is a linear function of Ge for positive and negative values of C_z . Further, the absence of Q indicates that, the increasing Gebhart number in the fluid medium slightly stabilizes the convection process, since; Ge increases the critical vertical Rayleigh number (R_z) and thereby delays the onset of instability in the flow regime. When the concentration-based internal heat generation is interposing to the fluid medium, the critical value of R_z is diminished for positive C_z (refer Fig. 6). For $Q = 0$ the profile is linear, and becomes monotonically nonlinear for $Q = 1$. However, at $Q = 2$ profile is oscillatory in nature indicating strong non-linearity and a more complex interplay between heat generation and stability characteristics for $Q > 1$. Conversely, in Fig. 7 with a negative value of C_z , the critical value of R_z is initially elevated with increment in Q (to 5) exhibiting an oscillatory topology and thereafter with further increment ($Q = 10$) it is reduced and moreover the profile is a linear decay not linear ascent at the highest value of Q . Maximum heat generation in this case therefore induces destabilization in the regime since it reduces the critical Rayleigh number corresponding to the onset of instability. The response is therefore much more complex for the case where mass diffusion is dominant at the lower boundary i.e. negative C_z , as compared with the other case where mass diffusion is dominant at the upper boundary (positive C_z , Fig. 6). This situation suggests that, the nature of the boundary condition at the plates also contributes significantly to the onset of stability in addition to the heat generation effect. In geothermal systems this is a critical issue since bounding strata can be porous and mass diffusion can be variable also [44]. Furthermore, in Fig. 6 increasing viscous dissipation i.e. higher Gebhart number (Ge) consistently boosts the critical vertical Rayleigh number, whereas in the Fig. 7 as explained, this pattern is only achieved for $Q = 0$ and $Q = 5$, not the maximum heat generation case of $Q = 10$. A dual response is therefore computed for negative C_z values in the Hadley-Prats flow. However, for the higher Gebhart number and concentration-based internal heat generation values, destabilization occurs more slowly in the flow regime. Increasing value of Q slightly decreases the critical value of R_z with rising viscous heating parameter Ge in the case $C_z > 0$ but as elucidated earlier, more complex changes occur for the case of $C_z < 0$ are demonstrated in Figs. 6 and 7.

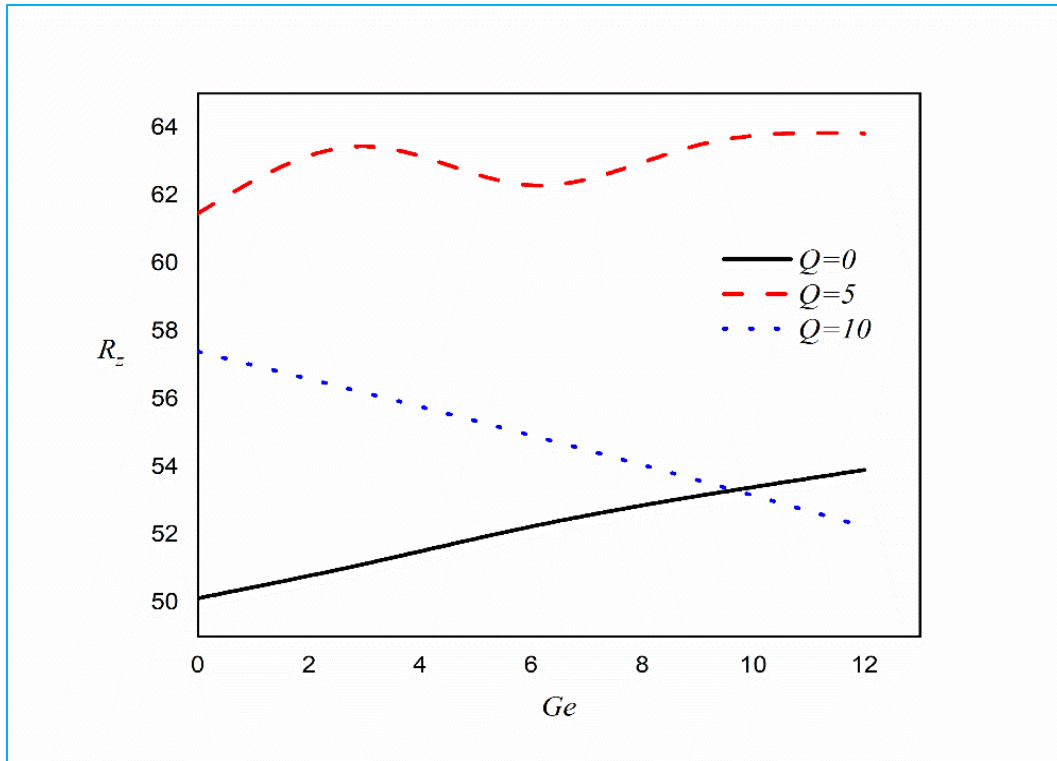


Figure 7: Deviations of R_z with Ge at $R_x = C_x = 5, R_y = C_y = 0, M = 2, Le = 10, C_z = -5$.

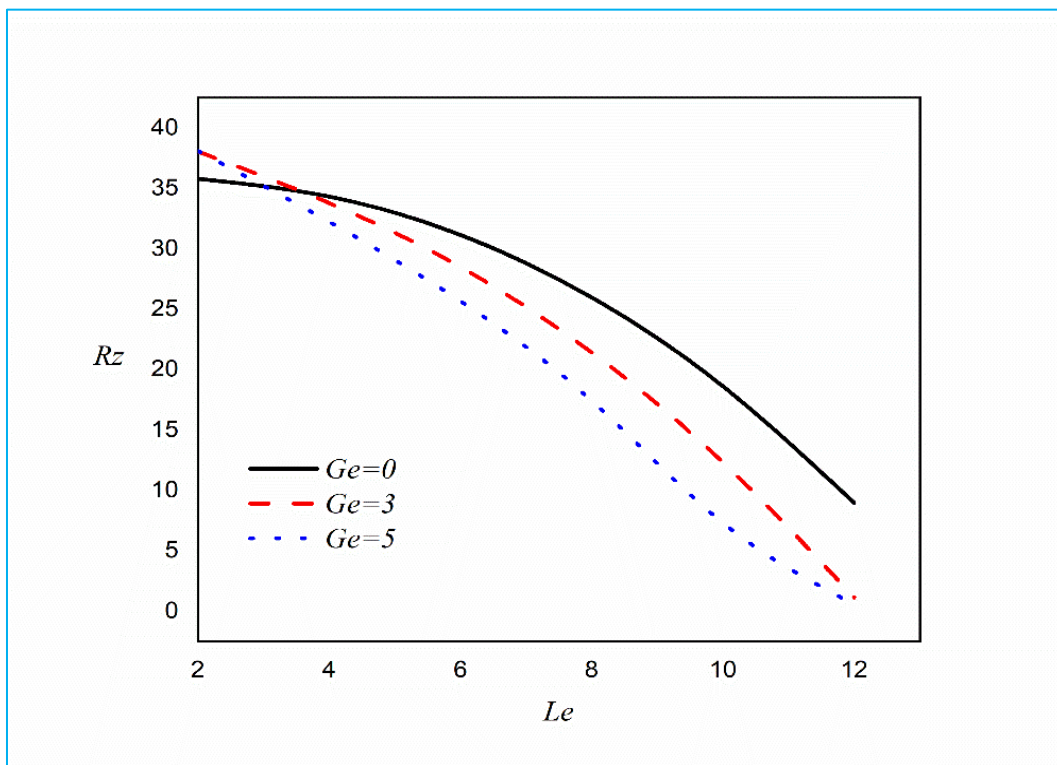


Figure 8: Deviations of R_z with Le at $R_x = C_x = 5, R_y = C_y = 0, M = 5, Q = 1$ and $C_z = 5$.

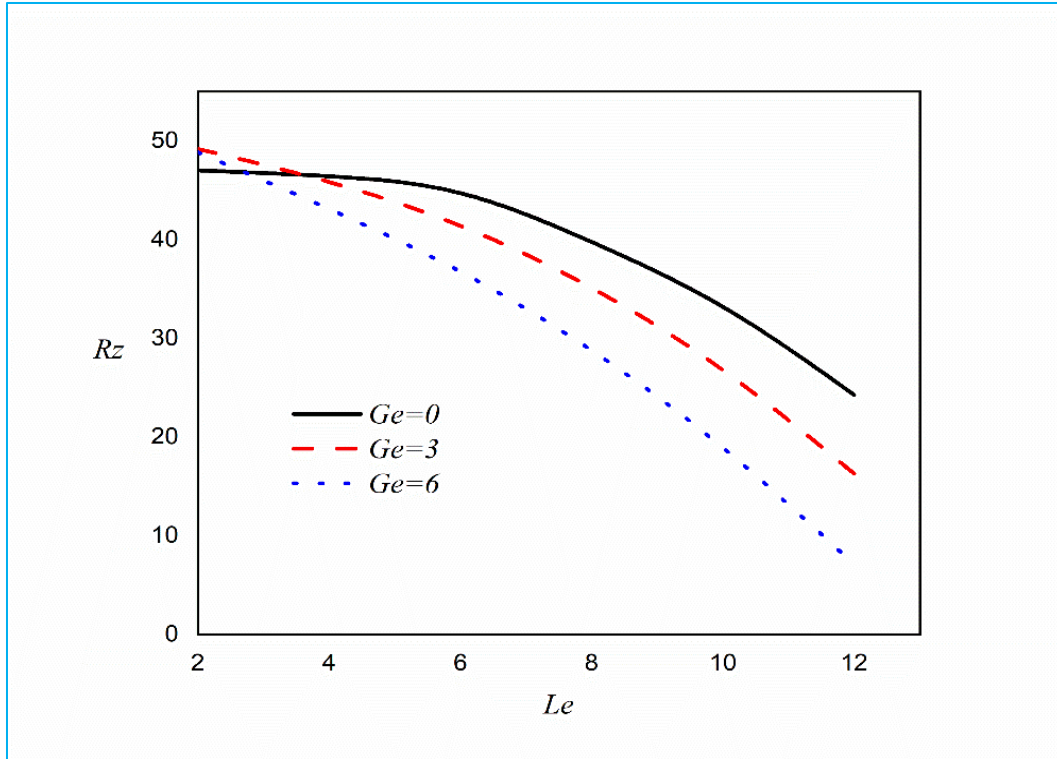


Figure 9: Deviations of R_z with Le at $R_x = C_x = 5$, $R_y = C_y = 0$, $M = 5$, $Q = 1$, $C_z = -5$.

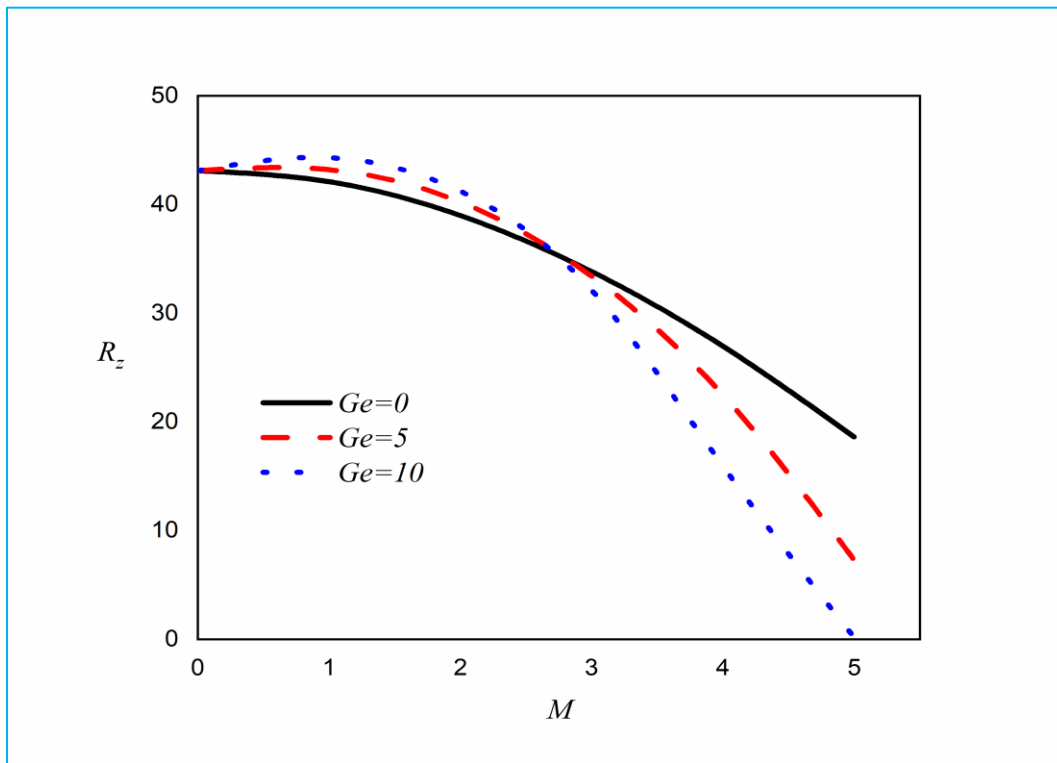


Figure 10: Deviations of R_z with M at $R_x = C_x = 5$, $R_y = C_y = 0$, $Le = 10$, $Q = 1$, $C_z = 5$.

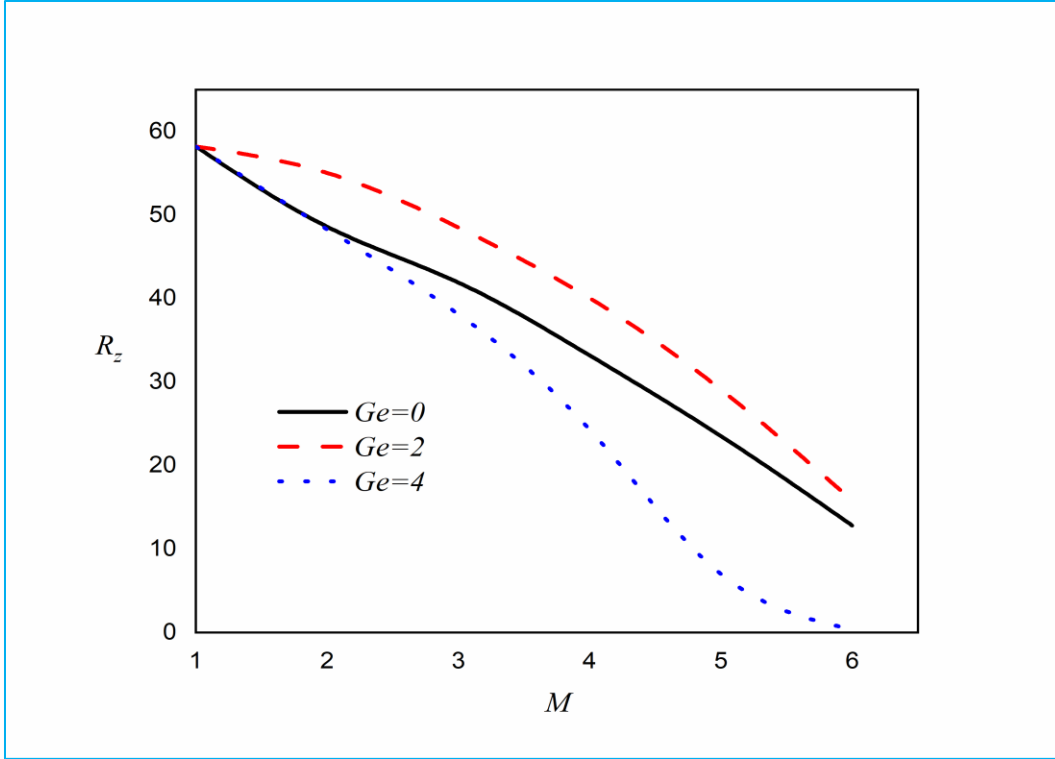


Figure 11: Deviations of R_z with M at $R_x = C_x = 5$, $R_y = C_y = 0$, $Le = 10$, $Q = 1$, $C_z = -5$.

Figures 8 and 9 illustrate the effect of Gebhart number Ge on critical vertical Rayleigh number, R_z with the collective variations in Lewis number Le for both negative and positive values of C_z . Figure 8 indicates that for vanishing viscous heating ($Ge = 0$) the critical value of R_z exhibits a diminishing behaviour with rising Le and fluid flow become more unstable (since the threshold for instability is lowered with a reduction in critical Rayleigh number). Further, in the presence of Ge the critical value of R_z is also decreased with an increment in Le for both $C_z < 0$ and $C_z > 0$. In both Figs. 8 and 9, we observed that, the response is in the form of monotonic decay i.e. a nonlinear depletion. Additionally, it is observed that, the value of R_z is reduced with enlargement in Gebhart number Ge . Also, overall vertical Rayleigh number R_z is reduced with an increase in viscous dissipation. Thus, the destabilization of Hadley-Prats flow is induced with the combined effects of higher Le (i.e. lower molecular diffusivity of the species) and higher Ge (i.e. greater internal frictional heating in the fluid). Linear stability shows that a boost in the Lewis number generally destabilizes the convection process for both positive and negative values of C_z in the presence of high viscous heating and concentration-based internal heat generation. As an additional note, it is important to mention that, the current simulations are confined to Newtonian

fluid behavior only. However the presence of multiple suspensions in geothermal fluid manifests in multiple species diffusion phenomena and these may also contribute to non-Newtonian behavior, for an instance couple stresses [45], which are neglected in the Navier-Stokes formulation. However, it is not considered in the present study, this aspect is under investigation and will be communicated in future studies by the authors.

Figures 10 and 11 describe the influence of viscous heating (Ge) on the vertical critical Rayleigh number R_z and M for both positive and negative values of C_z . In the absence of viscous heating ($Ge = 0$), rising M destabilizes the convection process. However, when viscous heating parameter ($Ge > 0$) is present, and for small M values, the fluid flow stabilized initially, but for the higher M values, the convection process destabilizes as illustrated in both Figs. 10 and 11. Further, the enhancing Ge diminish the R_z with rising M based on the linear stability analysis for both $C_z < 0$ and $C_z > 0$. This results proves that, the rising strength of mass flow parameter M , accelerate the onset of the destabilizing convection process. The present numerical simulations have generalized the previous studies to consider viscous dissipation, concentration-based internal heat generation, mass flow, horizontal temperature and solutal gradients and complex upper and lower boundary conditions. These results provide a good premise for the further extension to non-Newtonian fluid models [45] and also anisotropic porous medium [46].

From **Table 1**, it is also apparent that, an enlargement in the concentration-based heat generation parameter, C_z from negative to positive values, manifests in depletion with the R_z value. This suggests that, the porous medium thermo-solutal regime becomes unstable as C_z increases from negative to positive. **Table 2** summarizes the computations of R_z at $R_x = R_y = C_x = C_y = 0$, $Q = 0$, $Ge = 5$, $M = 0$ and $Le = 10$, for different values of C_z . From Table 2 it is clear that, increasing the values of C_z from negative to positive, the vertical values of thermal Rayleigh number decreases very quickly and this situation cause's strong destabilization in fluid flow in the infinite porous channel. From **Table 3** it is recorded that, the computations of R_z at $R_x = R_y = C_x = C_y = 0$, $C_z = -5$, $M = 0$ and $Le = 10$ for different values of concentration based internal heat source and viscous dissipation parameter for the case of linear stability theory. Here, for the negative value of vertical solutal Rayleigh number, the increasing concentration based internal heat source causes the increment of vertical thermal Rayleigh number and the fluid flow becomes more stable irrespective of viscous heating parameter.

From **Table 4** it is noticed that the computations of R_z at $R_x = R_y = C_x = C_y = 0, C_z = 5, M = 0$ and $Le = 10$, for the different values of concentration based internal heat source and viscous dissipation parameter for the case of linear stability theory. In this case, for the positive value of vertical solutal Rayleigh number, the increasing concentration based internal heat source causes the decay of vertical thermal Rayleigh number and the fluid flow becomes more unstable irrespective of the viscous dissipation parameter. Hence stronger destabilization will occur due to the increasing concentration based internal heat source for the positive value of vertical solutal Rayleigh number. This can be revealed by noting that the internal heat source, which depends on the concentration, elevates the overall temperature of the system, thereby prompting the system to enter an onset mode.

Table 1. Critical R_z at $R_x = R_y = C_x = C_y = 0, Q = 0, M = 0, Ge = 5$ and $Le = 10$.

C_z	30	20	10	10^{-5}	-5	-10	-15
R_z	9.478418	19.478424	29.478423	39.478406	44.478421	49.478423	54.541804
α	3.139999	3.139999	3.139999	3.139999	3.139999	3.139999	3.269999

Table 2. Critical R_z at $R_x = R_y = C_x = C_y = 0, Q = 5, M = 0, Ge = 0$ and $Le = 10$.

C_z	9	6	3	10^{-5}	-3	-6	-9
R_z	6.314146	17.370420	28.426524	39.478440	50.105116	60.484434	70.863554
α	3.110000	3.110000	3.110000	3.139999	3.399999	3.399999	3.399999

Table 3. Critical R_z at $R_x = R_y = C_x = C_y = 0, C_z = -5, M = 0$ and $Le = 10$.

Parametric values	Q	0	0.5	1	1.5	2
$Ge = 0$	R_z	44.478421	45.798117	47.097551	48.376765	49.635879
	α	3.1399	3.1899	3.239999	3.299999	3.349999
$Ge = 3$	R_z	46.9324	47.9821	48.3146	49.9244	50.5355
	α	3.1399	3.1899	3.1899	3.1999	3.1999
$Ge = 6$	R_z	47.5784	48.9066	49.7893	50.3998	51.2959
	α	3.1399	3.1499	3.1999	3.2999	3.2999

Table 4. Critical R_z at $R_x = R_y = C_x = C_y = 0$, $C_z = 5$, $M = 0$ and $Le = 10$.

Parametric values	Q	0	0.5	1	1.5	2
$Ge = 0$	R_z	34.391399	33.139790	31.797154	30.454501	29.111844
	α	3.1399	3.1100	3.1499	3.1500	3.1999
$Ge = 3$	R_z	35.2724	34.7871	33.9196	32.9294	31.9359
	α	3.1399	3.1399	3.1699	3.1999	3.1999
$Ge = 6$	R_z	36.9784	35.9005	34.7273	33.3478	32.2175
	α	3.1399	3.1499	3.1999	3.1999	3.1999

6.1. Validation

To validate the present solutions, authors have compared the current solutions with available existing results of Matta et al. [18] in the absence of viscous heating effect. This validation is clearly described in **Table 5**. It is clear from Table 5 table that, the present numerical solutions are excellently matching with the existing results of Matta et al. [18] and this fact confirms the accuracy of the current results reported in this article. Also, this fact confirms the high level of confidence in the present numerical solution methodology and the obtained results. Thus, authors believed that, this validation is sufficient enough to claim the accuracy of the current results.

Table 5. Validation of present solutions with the available results of Matta et al. [18] at critical R_z with $R_x = R_y = C_x = C_y = 0$, $Ge = 0$, $Q = 0$, $M = 0$ and $Le = 10$.

Parametric values	C_z	-30	-20	-10	10^{-5}	10	20	30
Results of Matta et al. [18]	R_z	69.478415	59.478415	49.478413	39.478301	29.478413	19.478414	9.478414
	α	3.141600	3.141600	3.141600	3.141600	3.141600	3.141600	3.141600
Present results	R_z	69.478343	59.478743	49.478396	39.476785	29.477789	19.478756	9.478454
	α	3.141600	3.141600	3.141600	3.141600	3.141600	3.141600	3.141600

7. Conclusions

A mathematical model is developed to investigate the thermo-convective instability in a horizontal permeable porous medium with concentration-based internal heat generation, mass flow, viscous dissipation, horizontal temperature and solutal gradients. The porous medium drag effects are evaluated in terms of Darcy flow model. A linear stability analysis of thermal and solutal convection mechanism in Hadley-Prats flow is conducted to examine the impacts of concentration-based heat source in addition to the other thermo physical effects on the onset of instability in the flow regime. The critical values of R_z are computed using Runge-Kutta scheme with shooting technique in MATLAB software for the several values of the physical parameters. A reasonable accuracy with previous results in the special case of vanishing viscous heating effect is achieved. The principal findings of the current study are summarized as follows:

- Increasing C_z from negative to positive values suppresses the critical vertical Rayleigh number R_z and this fact accelerates the onset of instability in the flow regime.
- Enhancing Lewis and Gebhart numbers strongly diminishes the critical vertical Rayleigh number and therefore destabilizes the Hadley-Prats flow in the porous medium.
- The flow regime becomes more stable with greater values of concentration-based heat source parameter Q and horizontal Rayleigh number.
- Destabilization of Hadley-Prats flow is induced for $C_z > 0$ and $C_z < 0$ with an increment in Gebhart number and concentration-based heat source parameter.
- An amplification in Lewis number strongly reduces the molecular diffusion relative to the thermal diffusivity and stabilizes the convection process for $C_z > 0$ and $C_z < 0$.
- Increasing concentration-based internal heat generation destabilizes the flow regime.
- Presence of horizontal mass flow yields destabilization effect in the porous medium.
- For the negative values of vertical solutal Rayleigh number with higher values of concentration based internal heat source parameter, the fluid system become more stable but for the positive values of vertical solutal Rayleigh number with higher values of concentration based internal heat source parameter, the fluid system is more unstable.

As documented earlier that, the present numerical investigation has produced some interesting insights of double-diffusive Hadley-Prats flow under the influence of porous medium with the direct consequence to the geothermal systems. However, in the present analysis, our attention has been confined to the Newtonian fluids with single phase behaviour and single diffusing species. Our future studies may include the analysis of nanofluids with species diffusion, hybrid-nano fluids, supercritical fluids and indeed other phenomena including thermal radiation, electromagnetic Joule heating (associated with ionic behaviour in saline geothermic), thermal stratification and thermal dispersion, and these physical effects are included in the available literature [47-53]. Efforts in this direction are underway and will be communicated soon.

Acknowledgements:

The authors wish to express their gratitude to the Editor and Reviewers who highlighted important areas for improvement in the earlier draft of this article. Their suggestions have served specifically to enhance the clarity and depth of the interpretation of results in the revised manuscript. The first author wishes to express his gratitude to Department of Science & Technology, Government of India, for granting DST-Inspire Fellowship (IF190169) and to the Department of Mathematics, Central University of Karnataka for providing the research facilities.

Notes on contributors:

Kallu Vetty Muhammed Rafeek has received his M.Sc in Mathematics with First Rank from Department of Mathematics, Central University of Karnataka, Kalaburagi and is presently pursuing his Ph.D. in Fluid Dynamics at Central University of Karnataka, Kalaburagi, India.

Gudal Janardhana Reddy is an Associate Professor & Head, Laboratory on Computational Fluid Dynamics, Department of Mathematics, Central University of Karnataka, Kalaburagi, India. He has received his M.Sc. degree in Mathematics from NIT Warangal and Ph.D. in Computational Fluid Dynamics from NIT Warangal, India. His working area of interest includes the fluid dynamics, non-Newtonian fluids, porous media, MHD, entropy generation analysis, supercritical fluids, turbulent flows and stability analysis.

Anjanna Matta is an Associate Professor in the Department of Mathematics, Faculty of Science & Technology, The ICFAI Foundation for Higher Education, Hyderabad, India. He has received his M.Sc. in Mathematics from NIT Warangal, M. Tech. from IIT Madras and PhD from IIT Hyderabad, India. His area of research interest includes stability analysis, fluid mechanics and porous medium.

Hussain Basha is an Assistant Professor (Contractual) in the Department of Mathematics, Government Degree College & PG Centre, Sindhanur, Karnataka, India. He has received his B.Sc degree from Gulbarga University with Second Rank, M.Sc in Mathematics from Gulbarga University with First Rank and PhD in Computational Fluid Dynamics from the Department of Mathematics, Central University of Karnataka, Kalaburagi, India. His area of research interest includes CFD, supercritical fluids, turbulent flows and non-Newtonian fluids.

Osman Anwar Bég CENG FIMECHE CMATH FIMA is a Professor and Director-Multi-physical Engineering Sciences Group (MPESG), Aeronautical/Mechanical Engineering Department, Corrosion/Coating Lab; SEE Bldg, Salford University, Manchester M54WT, UK. His broad research area interest includes heat transfer, non-Newtonian fluids, electrofluid mechanics, squeezing flow, porous media, magneto-hydrodynamics, aerodynamics, FSI and nanofluids.

Disclosure statement:

No potential conflict of interest was reported by the authors.

Nomenclature

d	Height of the porous layer.
D_m	Solutal diffusivity.
g_0	Acceleration due to gravity.
K	Permeability.
k_m	Thermal conductivity.
Le	Lewis number.
P	Dimensionless pressure.
M	Dimensionless Peclet number.

R_x, R_y	Horizontal thermal Rayleigh numbers.
C_x, C_y	Horizontal solutal Rayleigh numbers.
R_z	Vertical thermal Rayleigh number.
C_z	Vertical solutal Rayleigh number.
q	Dimensionless velocity.
C	Dimensionless concentration.
Q	Dimensionless heat source.
t	Dimensionless time.
u, v, w	x, y, z Components of dimensionless velocities.
Ge	Gebhart number (viscous heating parameter)

Greek symbols

α	Dimensionless overall wave number.
α_m	Thermal diffusivity.
$(\beta_{\theta_x}, \beta_{\theta_y})$	Horizontal thermal gradient vector.
$(\beta_{C_x}, \beta_{C_y})$	Horizontal solutal gradient vector.
γ_θ, γ_C	Thermal and solutal expansion coefficients.
θ	Dimensionless temperature.
ρ	Density.
\emptyset	Porosity.

Subscripts

f	Fluid region.
m	Porous medium.
s	Steady state.

Superscripts

'	Dimensional variables.
—	Disturbance quantities.

References

- [1] Chen F, Chen, CF, Pearlstein AJ. Convective instability in superposed fluid and anisotropic porous layers. *Phys Fluids A*. 1991;3(4): 556-565.
- [2] Bendrichi G, Shemilt LW. Mass transfer in horizontal flow channels with thermal gradients. *Can J Chem Eng*. 1997;75(6); 1067-1074.
- [3] Straughan B. Nonlinear stability for thermal convection in a Brinkman porous material with viscous dissipation. *Transp Porous Media*. 2020;134: 303-314.
- [4] Anderson JD, Bollinger RE, Lamb DE. Gas phase controlled mass transfer in two phase annular horizontal flow, *AIChE*. 1964;10(5): 640-645.
- [5] Taslim ME, Narusawa U. Thermal stability of horizontally superposed porous and fluid layers. *J Heat Transf*. 1989;111(2):357-362.
- [6] Horton CW, Rogers FT. Convection currents in a porous medium. *J Appl Phy*. 1945;16: 367-370.
- [7] Lapwood ER. Convection of a fluid in a porous medium. *Proc. Cambridge Phil.Soc.*, 1948;44(4):508-521.
- [8] Nield DA. Convection in a porous medium with inclined temperature gradient: additional results. *Int J Heat Mass Transf*. 1994;37(18):3021-3025.
- [9] Barletta A, Celli M, Nield DA. Unstable buoyant flow in an inclined porous layer with an internal heat source. *Int J Therm Sci*. 2014;79:176-182.
- [10] Nield DA, Bejan A. *Convection in Porous Media*. Springer, New York: 2013.
- [11] Hill AA. Double-diffusive convection in a porous medium with a concentration based internal heat source. *Proc.R. Soc.A.*, 2005;461:561-574.
- [12] Weber JE. Convection in a porous medium with horizontal and vertical temperature gradients. *Int J Heat Mass Transf*. 1974;17(2), 241-248.
- [13] Ingham DB, Pop I. *Transport Phenomena in Porous Media*. Pergamon, Oxford, 1998.
- [14] Vafai K. *Handbook of Porous Media*. CRC Press, Boca Raton, Florida: 2005.

- [15] Nield DA, Manole DM, Lage JL. Convection induced by inclined thermal and solutal gradients in a shallow horizontal layer of a porous medium. *J Fluid Mech.* 1993;257:559-574.
- [16] Manole DM, Lage JL, Nield DA. Convection induced by inclined thermal and solutal gradients, with horizontal mass flow, in a shallow horizontal layer of a porous medium. *Int J Heat Mass Transf.* 1994;37:2047-2057.
- [17] Barletta A, Nield DA. Instability of Hadley-Prats flow with viscous heating in a horizontal porous layer. *Transp Porous Media.* 2010;84:241-256.
- [18] Matta A, Narayana PAL, Hill AA. Double diffusive Hadley-Prats flow in a horizontal porous layer with a concentration based internal heat source. *J Math Anal Appl.* 2017;452(2):1005-1018.
- [19] Matta A, Narayana PAL, Hill A A. Double diffusive Hadley-Prats flow in a porous medium subject to gravitational variation. *Int J Thermal Sci.* 2016;102:300-307.
- [20] Barletta A, Nield DA. On Hadley flow in a porous layer with vertical heterogeneity. *J Fluid Mech.* 2012;710:304-323.
- [21] Gebhart B. Effects of viscous dissipation in natural convection. *J. Fluid Mech.* 1962;14(2): 225-232, 1962.
- [22] Turcotte DL, Hsui AT, Torrance KE, Schubert G. Influence of viscous dissipation on Benard convection. *J Fluid Mech.* 1974;64(2):369-374.
- [23] Barletta A, Storesletten L. Viscous dissipation and thermo convective instabilities in a horizontal porous channel heated from below. *Int J Thermal Sci.* 2010;49:621-630.
- [24] Nield DA, Barletta A, Celli M. The effect of viscous dissipation on the onset of convection in an inclined porous layer. *J Fluid Mech.* 2011;679:544-558.
- [25] Barletta A, Nield DA. Thermo-solutal convective instability and viscous dissipation effect in a fluid-saturated porous medium. *Int J Heat Mass Transf.* 2011;54(7-8):1641-1648.
- [26] Deepika N, Narayana PAL. Linear stability of double diffusive convection of Hadley-Prats flow with viscous dissipation in a porous media. *Procedia Eng.* 2015;127:193-200.
- [27] Deepika N, Narayana PAL. Effects of viscous dissipation and concentration based internal heat source on convective instability in a porous medium with through flow. In: *Conference World Academy of Science, Engineering and Technology.* 2015; 9(7): 1-5.

- [28] Ene HI, Palencia ES. On thermal equation for flow in porous media. *Int J Eng Sci.* 1982;20(5): 623-630.
- [29] Barletta A, Celli M, Rees DAS. The onset of convection in a porous layer induced by viscous dissipation: A linear stability analysis. *Int J Heat Mass Transf.* 2009;52:337-344.
- [30] Thirlby R. Convection in an internally heated layer. *J Fluid Mech.* 2013;44:673-693.
- [31] Tveitereid M, Palm E. Convection due to internal heat sources. *J Fluid Mech.* 1976;76:481-499.
- [32] Schwiderskei W, Schwabh JA. Convection experiments with electrolytically heated fluid layers. *J Fluid Mech.* 1971;48(4):703-719.
- [33] Tritton J, Zarraga MN. Convection in horizontal layers with internal heat generation. *J Fluid Mech.* 1967;30(1):21-31.
- [34] Parthiban C, Patil PR. Effect of non-uniform boundary temperatures on thermal instability in a porous medium with internal heat source. *Int Commun Heat Mass Transf.*, 1997;22:683-692.
- [35] Parthiban C, Patil PR. Thermal instability in an anisotropic porous medium with internal heat source and inclined temperature gradient. *Int. Commun Heat Mass Transf.*, 1997;24(7):1049-1058.
- [36] Matta A, Narayana PAL, Hill A. A. Nonlinear thermal instability in a horizontal porous layer with an internal heat source and mass flow. *Acta Mech.* 2016;227:1743-1751.
- [37] Matta A. Mono-diffusive Hadley-Prats flow in a horizontal porous layer subject to variable gravity and internal heat generation. *Heat Transf.* 2019;48(4): 1399-1412.
- [38] Deepika N, Matta A, Narayana PAL. Effect of throughflow on double diffusive convection in a porous medium with concentration based internal heat source. *J Porous Media.* 2016;19(4): 303-312.
- [39] Krishnamurti R. Convection induced by selective absorption of radiation: a laboratory model of conditional instability. *Dyn Atmos Ocean.* 1997;27:367-382.
- [40] Gebhart B, Jaluria Y, Mahajan RL, Sammakia B. Buoyancy-induced flows and transport, hemisphere, Washington: 1988.

- [41] Guo J, Kaloni PN. Nonlinear stability and convection induced by inclined thermal and solutal gradients. *Z Angew Math Phys*. 1995;46:645-654.
- [42] Kaloni PN, Qiao Z. Non-linear stability of convection in a porous medium with inclined temperature gradient. *Int J Heat Mass Transf*. 1997;40:1611-1615.
- [43] Kaloni PN, Qiao Z. Nonlinear convection induced by inclined thermal and solutal gradients with mass flow. *Contin Mech Thermodyn*. 2000;12:185-194.
- [44] Kaloni PN, Qiao Z. Non-linear convection in a porous medium with inclined temperature gradient and variable gravity effects. *Int J Heat Mass Transf*. 2001;44(8):1585-1591.
- [45] Kaloni PN, Lou JX. Nonlinear convection of a viscoelastic fluid with inclined temperature gradient. *Contin Mech Thermodyn*. 2005;17:17–27.
- [46] Reshmi D, Murthy PVS. The onset of convective instability of horizontal throughflow in a porous layer with inclined thermal and solutal gradients. *Phys Fluids*. 2018;30(7):074104-19.
- [47] Bhadauria BS. Double-diffusive convection in a saturated anisotropic porous layer with internal heat source. *Transp Porous Media*. 2012;92:299-320.
- [48] Yadav D, Lee D, Che HH, Lee J. The onset of double-diffusive nanofluid convection in a rotating porous medium layer with thermal conductivity and viscosity variation: a revised model. *J Porous Media*. 2016;19(1):31-46.
- [49] Yadav D, Wang J. Convective heat transport in a heat generating porous layer saturated by a non-Newtonian nanofluid. *Heat Transf Eng*. 2018;44:1363-1382.
- [50] Yadav D. Numerical solution of the onset of Buoyancy-driven nanofluid convective motion in an anisotropic porous medium layer with variable gravity and internal heating. *Heat transf*. 2020;49(3):1170-1191.
- [51] Capone F, Gentile M, Hill AA. Double-diffusive penetrative convection simulated via internal heating in an anisotropic porous layer with throughflow. *Int J Heat Mass Transf*. 2011;54(7-8):1622-1626.
- [52] Yadav D, Awasthi MK, Al-Siyabi M, Al-Nadhairi S, Al-Rahbi A, Al-Subhi M, Ragoju R, Bhattacharyya K. Double diffusive convective motion in a reactive porous medium layer saturated by a non-Newtonian Kuvshiniski fluid. *Phy Fluids*. 2022;34(2):024104.

[53] Yadav D, Al-Siyabi M, Awasthi MK, Al-Nadhairi S, Al-Rahbi A, Al-Subhi M, Ragoju R, Bhattacharyya K. Chemical reaction and internal heating effects on the double diffusive convection in porous membrane enclosures soaked with Maxwell fluid. *Membranes*. 2012;12(3):338-364.